

Problem Set #2 Physics 728 Spring 2012

- 1) Derive the solution for the s-wave scattering phase shift in the low energy limit for an attractive square well potential ($V(r) = -|V_0|$ for $r \leq R$ and $V(r) = 0$ $r > R$).
here I meant total, elastic, and inelastic cross sections
- 2) Derive expressions for the partial wave sums of the total, absorptive/inelastic cross sections (σ) in terms of the Partial Wave Scattering Matrix Elements S_l and associated magnitudes η_l and phase shifts.
- 3) From B & D: Do Problem 12 below. Additionally, under what conditions for the values of the phase shifts will these terms dominate the angular distribution of the phase shifts?
- 4) Either do B & D Problem 11 below, (ignore the statement about "single δ_1 phase shift" and ignore spin considerations), or pick any number > 3 of non-zero phase shifts for any l values (need not be for just s,p, or d waves) and use the macro provided on the web site to plot the angular distribution (feel free to plot as $d\sigma/d(\cos\theta)$).
- 5) Read the first paper "Justification for ..." in the attached pages (excluding APPENDIX), as well as the first 4 pages of the second paper "Application of ...". Answer the following questions:
 - a) How does Eq (2) in the first paper for the phase shift compare to the conditions we described for minima and maxima for a given phase shift?
 - b) Explain/Derive Equations (3),(4), and (5), in the first including the limits on the sum over l values, and the relation between the η_l discussed there and the η_l used in class/B&D/Vogt.
 - c) Relate figure 5 of the first paper to Figure 1 of the second paper.

- (11) If both $\tilde{l} = \tilde{0}$ and $l = \tilde{1}$ waves contribute to n-p scattering, evaluate the scattering angle dependence of the differential elastic scattering cross section in the simplifying assumption of a single δ_1 phase shift. Plot the expected cross section as a function of scattering angle assuming $\delta_0 = 45^\circ$ and $\delta_1 = 30^\circ$.
- (12) Suppose that in an elastic scattering experiment between two structureless particles the center-of-mass differential cross section may be represented by

$$\frac{d\sigma}{d\Omega} = A + B P_1(\cos\theta) + C P_2(\cos\theta) + \dots$$

Express the coefficients A , B and C in terms of the phase shifts δ_l .

Justification of a Simple Ramsauer Model for Neutron Total Cross Sections

S. M. Grimes,* J. D. Anderson, R. W. Bauer,† and V. A. Madsen‡

Lawrence Livermore National Laboratory, P.O. Box 808, Livermore, California 94551

Received December 17, 1997

Accepted April 20, 1998

Abstract—The simple nuclear Ramsauer model has been used successfully to fit neutron total cross sections for more than four decades but has not been widely used because the foundations of the model seem so unrealistic. A diffraction model calculation with the inclusion of refraction and optical model calculations are shown to validate the use of this simple nuclear Ramsauer model for neutron total cross sections in the neutron energy region of 6 to 60 MeV. This model yields a simple formula for parameterizing the energy dependence of the neutron total cross section.

I. INTRODUCTION

The nuclear Ramsauer model was proposed by Lawson¹ more than 40 yr ago as a way of understanding variations in neutron total cross sections. Peterson² applied this model in detail and was able to fit quantitatively a large number of neutron total cross sections in the 6- to 60-MeV energy region. Although successful in describing many experimental results, the foundations of the model seemed so unrealistic that it was not widely used. As applied by Peterson,² it utilized the assumption that the scattering phase shifts were all equal, independent of angular momentum. This was equivalent to assuming that the nucleus looked like a right circular cylinder, i.e., a "slug model," with the beam incident along the symmetry axis. Intuitively, this seemed unrealistic. Franco³ used the Glauber⁴ approximation and evaluated the Ramsauer model by integrating over realistic path lengths as a function of impact parameter for a spherical geometry. Franco³ demonstrated that the assumption of equal phase shifts was not required but that only the average value of the phase shifts as a function of angular momentum l for a given energy needed to vary slowly with energy. However, because his model did not include refraction at the

nuclear surface, these calculations actually yield poor fits to the oscillations in the data.

More recently, the Ramsauer model was extended to include neutron spin-spin interactions,⁵ and subsequently an isospin dependent interaction was added.⁶ With this latter extension, the model was able to fit neutron total cross sections to a few percent and to fit the differences in total cross sections for adjacent isotopes.

The purpose of this paper is to demonstrate the physical basis for the success of this simple Ramsauer model and to show that the deficiencies in previous Glauber calculations were due to the neglect of refraction for neutron energies of 6 to 60 MeV.

We begin by reviewing the basis of the nuclear Ramsauer model and by showing how well it fits experimental data. We then extend the Glauber model to include refraction, and we show that the average path in nuclear matter closely approximates $2R$. We present the results of optical model calculations that highlight the similarities and differences between the simple Ramsauer model and realistic calculations. We also discuss potential advantages of this simple model for simulating large quantities of nuclear data for applications. A preliminary report of this analysis has been presented in Ref. 7.

II. REVIEW OF RAMSAUER MODEL

The basic picture of the nuclear Ramsauer effect² in neutron total cross sections is shown schematically in

*Permanent address: Ohio University, Department of Physics, Athens, Ohio 45701.

†E-mail: bauer2@llnl.gov

‡Permanent address: Oregon State University, Department of Physics, Corvallis, Oregon 97331.

Fig. 1. A neutron wave is incident on a nucleus represented by a square well potential of radius R . Interference between the part of the wave that has traversed the nucleus and the part that has gone around causes oscillations in the total cross section.

The first application of a Ramsauer-type model was by Lawson¹ in 1953. He calculated the phase shift associated with the passage of a neutron through a slab of nuclear material with a real attractive potential V , which was small compared with the neutron energy. From this he deduced those energies at which the neutron total cross section would be a maximum, i.e., phase shifted by odd multiples of π . He concluded that the agreement with data was as good as could be expected given the crudeness of the calculation.

Peterson² evaluated the equivalent phase shift for a spherical geometry and obtained

$$\beta = \frac{4n}{3} (k_{in} - k_{out})R, \quad (1)$$

where $4(R/3)$ is the average chord length through a sphere; n is a number somewhat larger than 1, allowing for the path length increase inside the nucleus due to refraction effects; and k_{in} and k_{out} are the neutron wave numbers corresponding to Fig. 1. As already shown by Lawson,¹ the condition for a maximum cross section is maximum destructive interference between the two wave components; i.e.,

$$\beta = \frac{4n}{3} R(k_{in} - k_{out}) = m\pi, \quad (2)$$

$$m = 1, 3, 5, \dots, \text{odd}$$

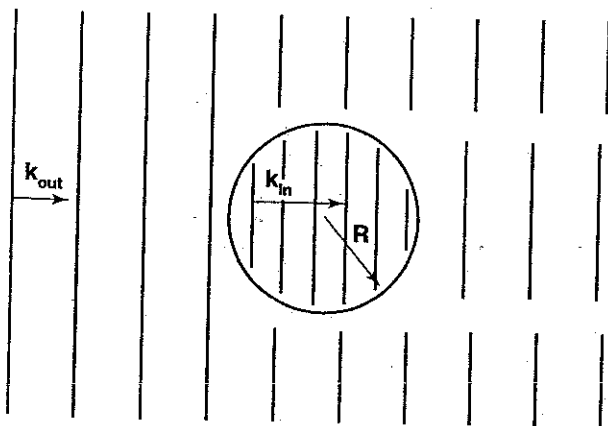


Fig. 1. Schematic representation of the Ramsauer process. A neutron wave is incident on the nucleus represented by a square well potential of radius R . Interference between the part of the wave that has traversed the nucleus and the part that has gone around causes oscillations in the neutron total cross section.

Peterson² evaluated this phase shift using optical potentials then available to determine the index of refraction n , and his comparison with the existing low-energy neutron data is shown in Fig. 2. Peterson² also showed that the total neutron cross sections could be split into two components. The nonelastic cross section was well described by the black nucleus approximation

$$\sigma_{ne} = \pi(R + \lambda)^2, \quad (3)$$

where λ is the reduced neutron wavelength, and the elastic cross section oscillated about this value because of the Ramsauer-type interference. No detailed comparison of total cross sections was attempted because the model was thought to be too crude compared with optical model calculations that were available.

To make detailed cross-section comparisons, we begin with the assumption of a slug model; i.e., the nucleus is assumed to be a right circular cylinder with the beam incident along the symmetry axis. The 0-deg scattering amplitude is given by

$$f(0 \text{ deg}) = \frac{i}{2k} \sum_{l=0}^L (2l+1)(1 - e^{i\eta_l}). \quad (4)$$

Because all path lengths are equal, we can assume η_l is a constant independent of l . Summing over l from $l=0$ to kR , we obtain

$$f(0 \text{ deg}) = \frac{ik}{2} (R + \lambda)^2 (1 - \alpha e^{i\beta}), \quad (5)$$

where we have replaced η_l by $-i \ln \alpha + \beta$. Using the optical theorem we obtain

$$\sigma_T = 2\pi(R + \lambda)^2 (1 - \alpha \cos \beta), \quad (6)$$

where the average behavior of the total cross section is described by $\sigma_T = 2\pi(R + \lambda)^2$ (the black nucleus approximation), and the effect of the interference or Ramsauer effect is reflected in the $(1 - \alpha \cos \beta)$ term. Here β is still the phase change in passing through the nucleus, and α , which is <1 , represents the absorption of the incident wave.

Franco³ was the first to attempt a theoretical evaluation of the Ramsauer model. Using the Glauber approximation, which totally neglects refraction by the nucleus, he was able to show that Eq. (2) is too restrictive and, in general, not correct. He showed that what was required was that the average value of the real part of $e^{i\eta_l}$ be a maximum (or minimum) and that, in general, the phase β was not an integer multiple of π . He also explicitly included the absorption process. Using the unmodified Glauber calculations (valid only at high energies) gave poor agreement with the data. By including a modified version more suitable to low neutron energies, he was able to achieve very good agreement with the location of the maxima and minima in the neutron cross sections. However, the low-energy structure in the

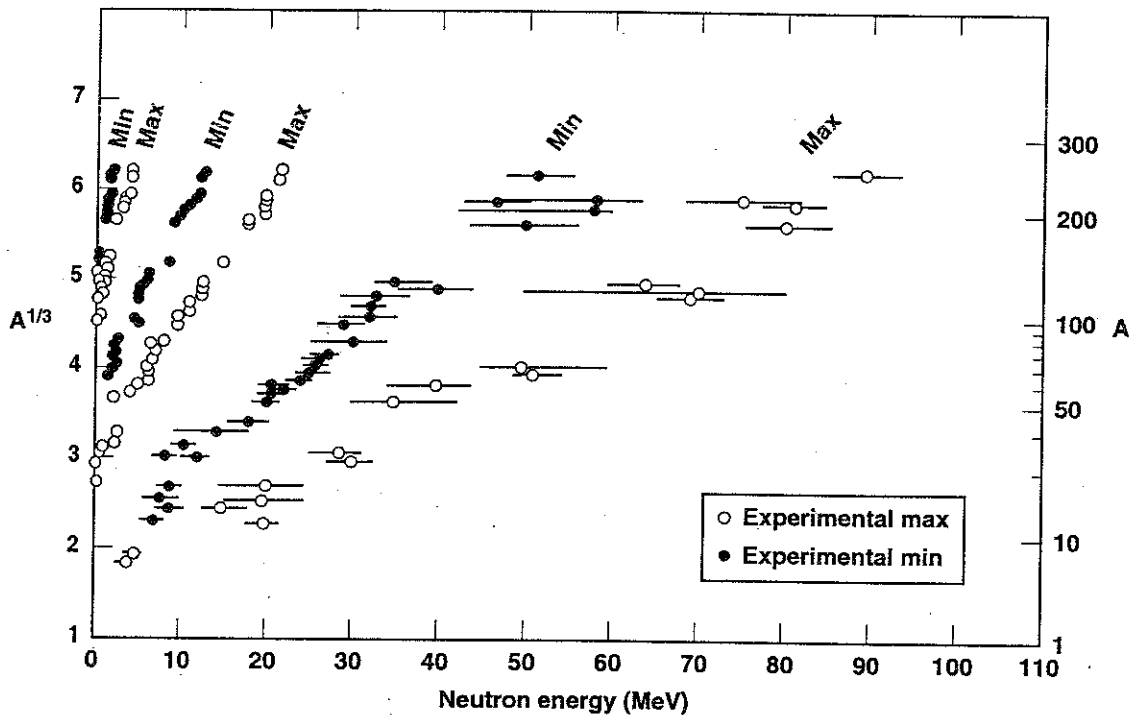


Fig. 2. The experimental maxima and minima in the neutron total cross sections are shown compared with the predictions of a simple Ramsauer model. (This is taken from Fig. 1 of Ref. 3.)

total cross sections was largely washed out, and no quantitative agreement was achieved. This is not surprising; detailed agreement was not the expected goal of this effort but rather a qualitative understanding of the underlying processes. More recently the interference properties of the nuclear Ramsauer effect were used by Gould et al.⁵ to elucidate the differences between the real and imaginary parts of the two-body spin-dependent force. Following Gould et al.'s work,⁵ Anderson and Grimes⁶ extended the Ramsauer model to include isospin. In addition, they attempted to describe precision total neutron cross sections using this model. In Fig. 3 we reproduced the comparison of the ^{140}Ce total cross section measured by Camarda, Phillips, and White⁸ and the Ramsauer model used in Ref. 6. Because Anderson and Grimes used the radius R taken from Peterson,² it is clear that with a small adjustment in this value, the data could have been fit at the 1 to 2% accuracy level. At that time, this level of agreement was considered fortuitous given the crude model, but it prompted our current investigation.

III. REFRACTION

In an attempt to get information about the importance of refraction, we investigate the simplest semiclassical model. We treat the refraction process of a wave

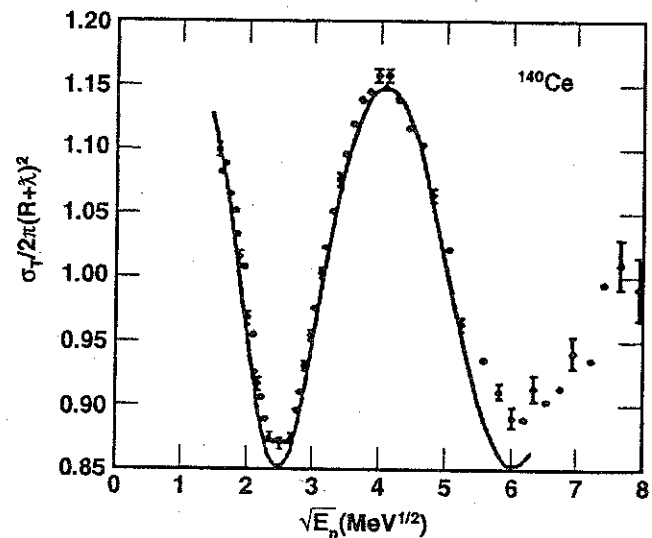


Fig. 3. The quantity $\sigma_T/2\pi(R + \lambda)^2$ is plotted versus the square root of the neutron bombarding energy. (R is taken from Ref. 2 as $1.35A^{1/3}$. The data are from Ref. 8. The phenomenological fit, from Ref. 6, is shown as the solid curve.)

incident on a uniform spherical potential. Furthermore, at each impact parameter, we treat the refraction process as if the ray of the projectile were bent by a plane of uniform nuclear matter tangent to the nuclear surface.

This leads to some minor inconsistencies but is still expected to give meaningful results. The ray then is assumed to travel in a straight line until it reaches the surface from inside. Reflections from inside the nuclear surface are ignored, assuming that the probability current in these rays is absorbed after reflection.

Matching the outside incident-plus-reflected wave of wave number k to the inside transmitted wave of (complex) wave number K gives a transmitted amplitude of

$$C = \frac{2Ak_{\perp}}{k_{\perp} + K_{\perp}}, \quad (7)$$

where A is the amplitude of the incident plane wave and k_{\perp} and K_{\perp} are the normal components of the respective wave numbers outside and inside the nucleus (as a function of impact parameter).

As shown in the Appendix, we can determine the direction of the transmitted ray where it emerges from the nucleus and thereby find the length of the chord of passage through the nucleus to be

$$l_c = \frac{2R}{1+m^2} \left[\frac{mb}{R} + \sqrt{1 - \frac{b^2}{R^2}} \right], \quad (8)$$

where R is the nuclear radius, b is the impact parameter, and m is the slope of the transmitted ray. Table I gives the length of the chord divided by the nuclear radius of the path through the nucleus as a function of impact parameter b and energy E . It is clear from the table that below 100 MeV refraction effects are very large. In the lower portion of this energy range, the nuclear-transit chord length is a large fraction of the nuclear diameter for all impact parameters up to the nuclear radius. This is in striking contrast to the Glauber model, for which the chord length $l_c = 2\sqrt{R^2 - b^2}$ goes to zero at impact parameter $b = R$. Because of the slow falloff of l_c as a function of b , the phase shift of the refracted wave (see Appendix),

$$\beta = (K - k\hat{n}_i \cdot \hat{n}_t) l_c, \quad (9)$$

TABLE I

Ratio of Chord Length to Radius

b/R	1 MeV	10 MeV	20 MeV	40 MeV	100 MeV
0	2.00	2.00	2.00	2.00	2.0
0.2	1.999	1.993	1.987	1.979	1.966
0.4	1.997	1.973	1.949	1.916	1.862
0.6	1.993	1.936	1.884	1.806	1.673
0.8	1.987	1.884	1.789	1.639	1.366
1.0	1.980	1.816	1.658	1.396	0.816

TABLE II

Ratio of Phase Shift to Radius

b/R	$E = 1$ MeV	$E = 10$ MeV	$E = 20$ MeV	$E = 40$ MeV	$E = 100$ MeV
0	2.678	1.920	1.543	1.097	0.418
0.2	2.683	1.922	1.541	1.090	0.411
0.4	2.701	1.933	1.537	1.070	0.392
0.6	2.734	1.958	1.537	1.040	0.357
0.8	2.797	2.026	1.565	1.012	0.302
1.0	3.023	2.473	1.995	1.314	0.326

is nearly independent of b for each energy, as can be seen from Table II. These calculations were for the large nucleus lead and will be discussed further in Sec. IV.

IV. OPTICAL MODEL CALCULATIONS

Peterson² was the first to compare the simple Ramsauer model result with optical model calculations. His intent was to demonstrate from these optical model calculations that the maxima in the neutron total cross sections came from significant contributions from a large number of partial waves, i.e., that it was a Ramsauer-type effect, not a single particle resonance. McVoy⁹ showed in detail that these maxima were due to a large number of phase shifts passing downward through 180 deg rather than upward as in a resonance. This conclusion of McVoy⁹ is the first statement that a large number of phase shifts have approximately the same value, hence supporting the validity of a simple Ramsauer model. With the inclusion of refraction in our diffraction model, the results suggest that in a Glauber calculation the nucleus behaves more like a right cylinder than a sphere, which also partially justifies our simple Ramsauer model.

We now make detailed comparisons with optical model calculations. The potential used is that of Rappaport, Kulkarni, and Finlay.¹⁰ We want a large variation in l to see if η_l can be replaced by a constant, so we choose a large nucleus lead. To reduce the total number of phase shifts to a tractable number for presentation, we assigned the neutron a zero spin to eliminate the spin-orbit splitting. The calculated $e^{i\eta_l}$ are shown in Fig. 4 for energies from 14 to 30 MeV. We observe that although η_l is by no means independent of l , the amplitudes for $l = 0$ to 6 rotate together; i.e., they have an average value that rotates at a relatively constant rate. Note this is exactly Franco's criterion for Ramsauer behavior; i.e., $Re\langle e^{i\eta_l} \rangle$ is periodic. The $l = 7, 8,$ and 9

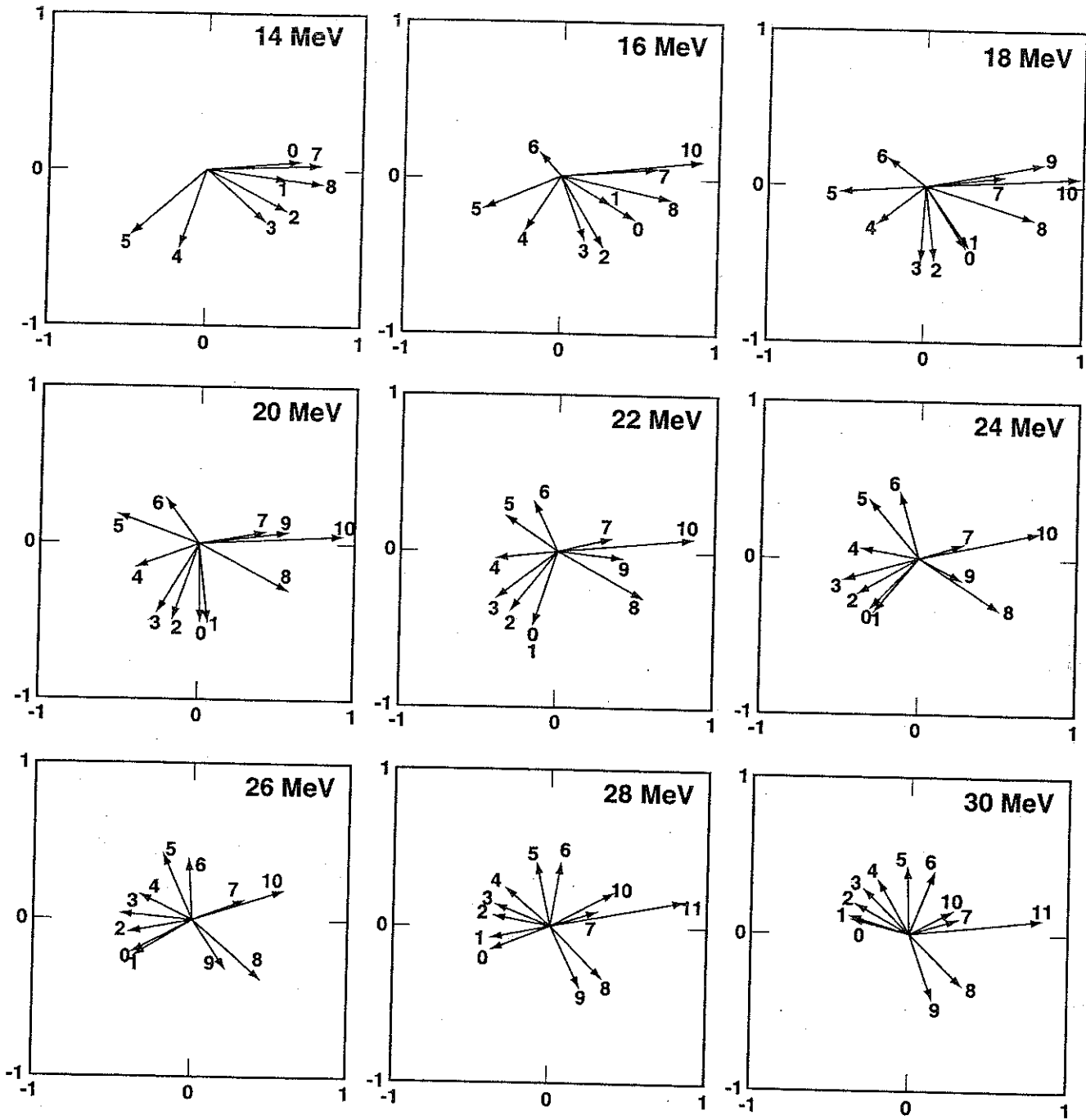
$e^{in\ell}$ ^{208}Pb Ohio Potential ($s=0$)


Fig. 4. The scattering matrix elements for neutron incident on lead are shown for several bombarding energies. The numbers in the figure indicate the angular momentum of the various partial waves. For simplicity, the neutron spin has been set to zero.

phase shifts, which correspond to the surface, rotate much more slowly as a function of bombarding energy. Note that $l = 7$ is about equal to kR at the edge of the nucleus for $E_n = 16$ MeV and is practically stationary for neutron energies from 16 to 30 MeV, while $l = 8$ and 9

rotate at about half the angular velocity of $l = 6$. In Fig. 5 we average the phase shifts shown in Fig. 4 with partial-wave cross-section weighting to show that they can be represented quite well by a single phase shift rotating slowly with energy.

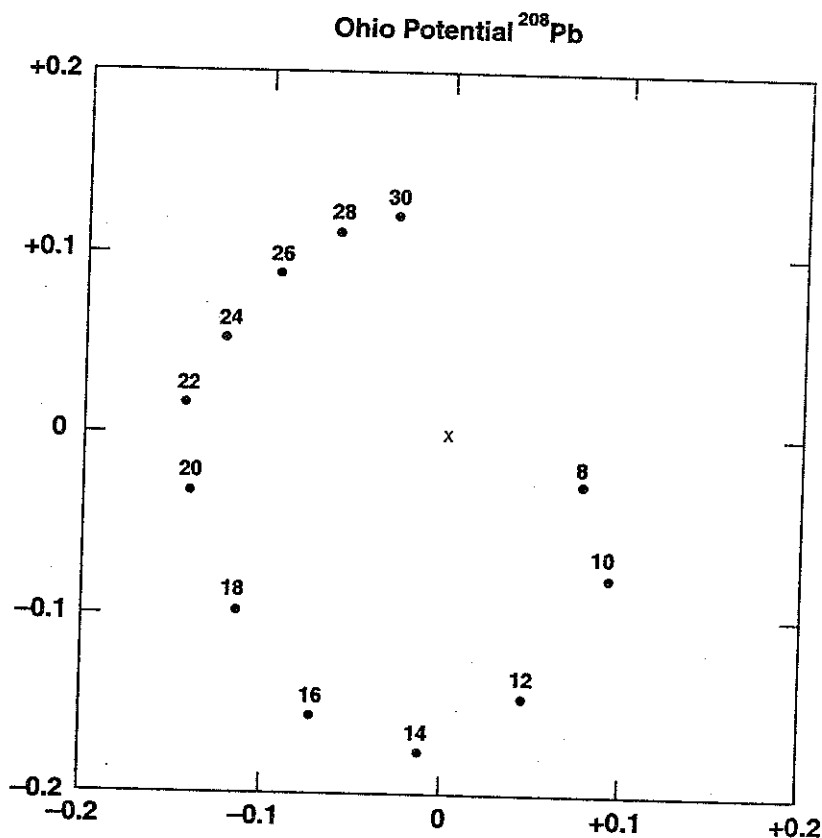


Fig. 5. The effective scattering matrix element, derived from Fig. 4, is shown as a function of neutron bombarding energy. This is to be compared with the Ramsauer single phase shift approximation. (Please note a change in scale from Fig. 4.)

In Table II we show the phase difference for various neutron energies and impact parameters from our diffraction calculations for lead. Assuming that the impact parameter scales as l , we find near constancy of the phase differences as a function of l at a given energy, in agreement with the optical calculations shown in Fig. 4.

We conclude that the Franco³ criterion for Ramsauer oscillations is well met but that our assumption that η_l is constant is a statement of average value; i.e., it can be replaced by $Re\langle e^{i\eta_l} \rangle$. In both of these cases, we neglected the nuclear surface. In Ref. 6 a surface term was added; however, it did not improve the fit to the actual neutron data compared with that obtained in Ref. 2. This would seem to be the statement that the simple Ramsauer form has ample flexibility in fitting data by choosing an appropriate energy dependence to β .

It is commonly assumed (Ref. 11) that the strength of the neutron absorption, i.e., the imaginary part of the optical potential, can be estimated from the magnitude of the oscillations in the neutron total cross section. From comparisons with cerium and lead calculations, we note that the α needed to fit the neutron cross sections using the simple Ramsauer model is a factor of 2 to 3 smaller than $\langle \alpha_l \rangle$ given by optical model calculations. This is be-

cause of appreciable cancellation resulting from the small but significant phase change as a function of l . It should be noted that Glauber calculations overestimate this averaging, and thus $\langle \alpha_l \rangle$ is a factor of 2 too small compared with the optical model estimate. We conclude that no detailed information on the magnitude of the absorptive potential can be extracted without recourse to optical model calculations.

V. CONCLUSIONS

We used a diffraction model to include the effect of path lengthening resulting from refraction and showed that the average effective path length of a low-energy neutron passing through the nucleus is $\sim 2R$. This approximation is fairly accurate for neutron energies from 6 to 60 MeV (see Table I). This seems to account partially for the success of the simple Ramsauer model in fitting precision neutron cross sections in this energy region. Detailed comparison with optical model calculations reveals that the precision of the fits also comes from the fact that the expectation value of the real part of the scattering

amplitude varies slowly and smoothly with energy. Thus, we conclude that this model may be robust in its ability to fit neutron total cross sections accurately.

The fact that a few parameters can fit the data, e.g., four in Ref. 6, implies that several of the parameters used in optical calculations are redundant. As is well known from optical model analysis, the principal dependence of the structure of the total cross section is on the product VR^2 . Furthermore, as pointed out by Johnson, Horen, and Mahaux,¹² we must make a dispersion correction to V at low energies if we wish to fit the low-energy structure precisely. Because this correction depends both on the magnitude of the imaginary potential and its energy dependence, the connection is sensitive to shell closures and cannot be extrapolated for use on nearby nuclei at low energy. Thus, the parameterization of the energy dependence of β is possibly an excellent pragmatic tool for representing cross sections where no data are available. The parameter α , as already pointed out, is only partially a measure of the absorptive potential but also includes the effect of phase shift averaging over l . The effects of the real potential on path lengthening, i.e., refraction, tend to make the path length much less dependent on l than in the Glauber approach.

We conclude that this simple model has sufficient justification to motivate its application in parameterizing total cross section systematics, which avoids the complexity of optical model calculations in applications over wide ranges of energy and atomic mass.

APPENDIX

We obtain the refraction angle by treating the incidence of a ray at impact parameter b as though the surface were a plane. A wave function of incident wave vector $k_i = k_{\perp} \hat{n}_{\perp} + k_{\parallel} \hat{n}_{\parallel}$ plus a reflected wave are matched, value and derivative, to a transmitted wave of wave number $K_t = K_{\perp} \hat{n}_{\perp} + k_{\parallel} \hat{n}_{\parallel}$ characteristic of the uniform nuclear medium. In these expressions, \hat{n}_{\perp} is the normal direction and \hat{n}_{\parallel} the transverse direction. The direction of the transmitted current density can be calculated to be

$$\hat{n}_t = \frac{k_{\parallel} \hat{n}_{\parallel} + \text{Re} K_{\perp} \hat{n}_{\perp}}{\sqrt{k_{\parallel}^2 + (\text{Re} K_{\perp})^2}}, \quad (\text{A.1})$$

so the cosine of the angle between the incident and refracted ray is

$$\hat{k}_i \cdot \hat{n}_t = \frac{k_{\parallel}^2 + k_{\perp} \text{Re} K_{\perp}}{\sqrt{k_{\parallel}^2 + k_{\perp}^2} \sqrt{k_{\parallel}^2 + (\text{Re} K_{\perp})^2}}. \quad (\text{A.2})$$

The inside wave number components were determined by the matching to be

$$k_{\parallel} = K_{\parallel} \quad (\text{A.3})$$

and

$$\text{Re} K_{\perp} \approx \sqrt{\frac{2\mu E}{\hbar^2} - k_{\parallel}^2 + \frac{2\mu V_0}{\hbar^2}}, \quad (\text{A.4})$$

where μ , E , V_0 , and \hbar are the projectile mass, projectile energy, nuclear potential well depth, and Planck's constant divided by 2π , respectively. For these calculations, we used V_0 (in mega-electron-volts) = 50–0.3E.

Using $k_{\parallel} = (b/R)k$ leads to the result

$$\begin{aligned} \hat{k}_i \cdot \hat{n}_t = & \sqrt{\frac{E}{E + V_0}} \left(\frac{b}{R}\right)^2 \\ & + \sqrt{1 - \left(\frac{b}{R}\right)^2} \sqrt{1 - \frac{E}{E + V_0}} \left(\frac{b}{R}\right)^2, \end{aligned} \quad (\text{A.5})$$

where E is the energy and V_0 the (positive) depth of the real nuclear potential. Next, we write the equation for the transmitted ray line in the x, y plane,

$$y = b - m\sqrt{R^2 - b^2} - mx, \quad (\text{A.6})$$

where x and y are the normal and transverse coordinates and

$$m = \frac{\sqrt{1 - (\hat{k}_i \cdot \hat{n}_t)^2}}{\hat{k}_i \cdot \hat{n}_t} \quad (\text{A.7})$$

is the magnitude of the slope of the chord of the transmitted ray. Equation (A.6) and the equation for the spherical nuclear surface in the reaction plane,

$$x^2 + y^2 = R^2, \quad (\text{A.8})$$

are solved simultaneously, giving the two roots

$$(x_1, y_1) = (-\sqrt{R^2 - b^2}, b) \quad (\text{A.9})$$

and

$$\begin{aligned} (x_2, y_2) = & \frac{1}{1 + m^2} (2mb + (1 - m^2)\sqrt{R^2 - b^2}, b(1 - m^2) \\ & - 2m\sqrt{R^2 - b^2}). \end{aligned} \quad (\text{A.10})$$

The first solution is the entry point of the ray, and the second is the exit point. The chord length of the transmitted ray in the nucleus is then the distance l_c between these two points, which can be calculated to be

$$l_c = \frac{2R}{\sqrt{1 + m^2}} \left[\frac{mb}{R} + \sqrt{1 - \frac{b^2}{R^2}} \right]. \quad (\text{A.11})$$

For $b = 0$, m is also 0, and Eq. (A.11) gives $l_c = 2R$, the nuclear diameter, as expected.

The phase shift (for a forward-scattered neutron) as an implicit function of impact parameter b is

$$\beta = (K - k_i \cdot \hat{n}_t) l_c, \quad (\text{A.12})$$

where k_i and \hat{n}_i are vectors in the k and K direction, respectively. Equation (A.12) can be interpreted as the phase of the refracted wave crossing the nucleus on the chord of length l_c minus the phase of a free-particle wave traversing the horizontal component of the same chord.

ACKNOWLEDGMENTS

This work was performed under the auspices of the U.S. Department of Energy by the Lawrence Livermore National Laboratory (LLNL) under contract W-7405-ENG-48. We also acknowledge the support of the LLNL Nuclear Data Group under Roger M. White for its support.

REFERENCES

1. J. D. LAWSON, "A Diffraction Effect Illustrating the Transparency of Nuclei to High Energy Neutrons," *Phil. Mag.*, **44**, 102 (1953).
2. J. M. PETERSON, "Neutron Giant Resonances—Nuclear Ramsauer Effect," *Phys. Rev.*, **125**, 955 (1962).
3. V. FRANCO, "Qualitative Aspects of Neutron-Nuclear Interaction and the Optical Model," *Phys. Rev. B*, **140**, 1501 (1965).
4. R. J. GLAUBER, *Lectures in Theoretical Physics*, Vol. I, p. 315, Interscience, New York (1959).
5. C. R. GOULD, D. B. HAASE, L. W. SEAGONDOLLAR, J. P. SODERSTRUM, K. E. NASH, M. B. SCHNEIDER, and N. R. ROBERSON, "Spin-Spin Potential in $N_{\text{pol}} + {}^{27}\text{Al}_{\text{pol}}$ and the Nuclear Ramsauer Effect," *Phys. Rev. Lett.*, **53**, 2371 (1986).
6. J. D. ANDERSON and S. M. GRIMES, "Nuclear Ramsauer Effect and the Isovector Potential," *Phys. Rev. C*, **41**, 2904 (1990).
7. A preliminary application of this model has been presented by R. W. BAUER, J. D. ANDERSON, S. M. GRIMES, and V. A. MADSEN, "Application of a Simple Ramsauer Model to Neutron Total Cross Sections," *Proc. Int. Conf. Nuclear Data for Science and Technology*, Trieste, Italy, May 19–24, 1997.
8. H. S. CAMARDA, T. W. PHILLIPS, and R. M. WHITE, "Neutron Absolute and Total Cross Section Difference Measurement in the Mass 140 Region," *Phys. Rev. C*, **29**, 2106 (1984).
9. K. W. MCVOY, "Giant Resonances and Neutron-Nuclei Total Cross Section," *Ann. Phys. (N.Y.)*, **43**, 91 (1967).
10. J. RAPAPORT, V. KULKARNI, and R. W. FINLAY, "A Global Optical Model Analysis of Neutron Elastic Scattering Data," *Nucl. Phys. A*, **330**, 13 (1979).
11. A. BOHR and B. MOTTELSON, *Nuclear Structure*, Vol. I, p. 166, Benjamin, New York (1969).
12. C. H. JOHNSON, D. J. HOREN, and C. MAHAUX, "Unified Description of the Neutron ${}^{208}\text{Pb}$ Mean Field Between -20 and $+165$ MeV from the Dispersion Relation Constraint," *Phys. Rev. C*, **36**, 2252 (1987).

Application of a Simple Ramsauer Model for Neutron Total Cross Sections

R. W. Bauer,* J. D. Anderson, S. M. Grimes,† D. A. Knapp
and V. A. Madsen‡

Lawrence Livermore National Laboratory, P.O. Box 808
Livermore, California 94551

Received December 17, 1997

Accepted April 20, 1998

Abstract—A companion paper presented arguments that support the applicability of a simple Ramsauer model to describe neutron total cross sections. Such a model yields a simple equation for the energy dependence of the cross section of a given nucleus and also allows extrapolation to nuclei of other A values. Fits of the Ramsauer form to very precise total cross sections recently measured over an extended energy range are presented. Very good fits are obtained for neutron energies between 6 and 60 MeV, suggesting that this approach will be useful for estimating cross sections in cases where experimental data are unavailable. Extension of this model to 120 MeV was only moderately successful.

I. INTRODUCTION

The nuclear Ramsauer model for neutron total cross sections has nearly a 50-yr history. In this model the neutron total cross section has been represented as the sum over contributions from a large number of partial waves of differing angular momentum. In analogy with the atomic Ramsauer analysis, the nuclear Ramsauer model assumes the phases of the various angular momenta to be the same, thus yielding a single average phase shift. Lawson¹ and Peterson² applied such a model to the analysis of neutron total cross sections. Subsequent study of this model³⁻⁶ verified that the maxima and minima in neutron total cross sections are not single particle resonances but are the result of the phase shifts of a number of partial waves varying at about the same rate with energy. Our companion paper⁷ studies the reasons for this behavior in detail, looking at the optical model predictions for the phase shift and examining semiclassical models for the various trajectories.

In this paper, we compare the predictions of the Ramsauer model with recent measurements of the total neutron cross sections for a number of elements.^{8,9} These data are highly precise (errors <2%) and span a wide energy range. Results of a preliminary application of the Ramsauer model in the limited energy range from 5.3 to 60 MeV have been reported at a recent conference.¹⁰

It should be noted that all comparisons in this paper are based on experimental data averaged in energy bins of width equal to 1% in energy. At low energies, the intrinsic resolution of the time-of-flight spectrometer was <1%, and fine structure, corresponding to resolved resonances and interference between a number of resonances, can be seen. Just as this fine structure does not appear in optical model fits, it is also not included in Ramsauer model expansions.

II. CALCULATIONS AND FITS

In the companion paper⁷ it is shown that for neutron bombarding energies <100 MeV and above the resonance region, the total cross section should have the form

$$\sigma_T = 2\pi(R + \lambda)^2(1 - \alpha \cos \beta), \quad (1)$$

*E-mail: bauer2@llnl.gov

†Permanent address: Ohio University, Department of Physics, Athens, Ohio 45701.

‡Permanent Address: Oregon State University, Department of Physics, Corvallis, Oregon 97331.

where

R = nuclear radius

λ = reduced wavelength of the neutron

α = parameter with the magnitude between 0 and 1

β = angle that gives the relative phase between the wave that passes through the nucleus and the wave that goes around the nucleus.

The black nucleus approximation assumes that all waves with impact parameter $b \leq R$ are completely absorbed. Inspection of the phase shift sum shows that such a situation gives an elastic cross section and an absorption cross section of $\pi(R + \lambda)^2$ each; this gives a total cross section of $2\pi(R + \lambda)^2$. This limit is achieved if $\alpha = 0$.

More generally, the α reflects not only the absorption but also the averaging of various phase shifts to produce an equivalent average phase shift. This makes α significantly less than would be estimated by calculating the absorption in passing through the nucleus.

In Ref. 7 it is shown that a semiclassical neutron ray with impact parameter b with respect to a spherical target nucleus of radius R refracts along a chord l_c inside the nucleus and suffers a phase shift with respect to a free neutron wave of

$$\beta = l_c(K_{in} - k_{out} \cdot \hat{n}_t) . \quad (2)$$

In Eq. (2) K_{in} and k_{out} are the inside and outside wave numbers, respectively, and \hat{n}_t is a unit vector in the direction of the transmitted ray. Numerical calculations shown in Table II of Ref. 7 show that this phase shift is nearly a constant as a function of impact parameter b and, therefore, approximately equal to the value at $b = 0$, giving for all b ,

$$\beta \approx 2R(K_{in} - k_{out}) = \frac{\sqrt{2m}}{\hbar} (2R)(\sqrt{V+E} - \sqrt{E}) , \quad (3)$$

where m is the neutron mass, \hbar is Planck's constant divided by 2π , and $R = r_0 A^{1/3}$.

In the nonrelativistic approximation, the phase angle β takes the form

$$\beta = cA^{1/3} \cdot (\sqrt{a + bE} - \sqrt{E}) . \quad (4)$$

The nuclear radius R in Eq. (3) has been explicitly included in $cA^{1/3}$ in Eq. (4). The quantity a corresponds to our optical potential V , and b includes the effects of the nonlocal energy correction. The quantities a , b , and c are the three fitting parameters to be determined [see Eq. (6) and subsequent text].

II.A. Reduction of σ_T to Dimensionless Units

The single most important criterion for the usefulness of the fitting process is the ability to scale over as

wide a range of nuclei, from light nuclei to the heaviest ones, and over as wide a range of energy as the model permits without adding numerous corrections. The large number of data points for each nucleus and the large number of nuclei for which experimental data are available made it possible to constrain the number of parameters easily. Although the most recent sets of precision data (Finlay et al.⁸ and Dietrich et al.⁹) are available over an energy range from 6 to 600 MeV, we shall limit our initial fits for total cross sections σ_T to an energy range from 6 to 60 MeV. As the first step we "reduce" the experimental cross sections to dimensionless quantities by dividing them by $2\pi(R + \lambda)^2$, i.e., the black nucleus approximation. This defines the reduced σ_r as

$$\sigma_r \equiv \frac{\sigma_T}{2\pi(R + \lambda)^2} = (1 - \alpha \cos \beta) . \quad (5)$$

We determine r_0 so that the normalized cross sections oscillate about unity because the Ramsauer model predicts that this quantity will be $1 - \alpha \cos \beta$. Examples of plots of σ_r as a function of \sqrt{E} are presented in Fig. 1. The values of r_0 for a wide range of nuclei have been derived from the plots of the type shown in Fig. 1 (σ_r to oscillate about unity). These values of r_0 are plotted as a function of $A^{1/3}$ in Fig. 2. It is to be noted that for the heavier nuclei, r_0 is fairly constant about the value of 1.37 ± 0.01 . However, as we move toward lighter nuclei, r_0 tends to increase monotonically toward higher values, approaching 1.45 for mass 40 (the lightest nucleus fitted by this procedure). These values can be expressed in form $R = r_1 A^{1/3} + 0.6$ with $r_1 = 1.27$ fm, which is quite consistent with the normal optical model radius of $1.27A^{1/3}$ and a surface thickness of 0.6 fm.

The deviation of r_0 from its nominal value for thorium and uranium (the heaviest nuclei fitted by this procedure) is explained by their static deformation. Since we are using a spherical model, the average cross section for the known deformation of these nuclei implies a 3 to 4% larger cross section than their spherical equivalent. Thus, in the cross-section reduction process, we expect r_0 to be 1.5 to 2% larger than neighboring spherical nuclei.

Table I summarizes the elements for which the nuclear total cross sections have been fitted in this investigation, together with the atomic numbers Z , the atomic mass A , and the radius r_0 determined by the cross-section reduction process.

II.B. Fits with Basic Ramsauer Model

Inspection of plots of the type presented in Fig. 1 permits us to determine the quantity α . The magnitude of α is determined by the size of the oscillation of the reduced cross section about unity. It is found that for essentially the whole range of nuclei fitted, α is constant within $\sim 10\%$. The average value of α is near 0.115 for the nuclei shown in Fig. 1. There is a slight tendency for

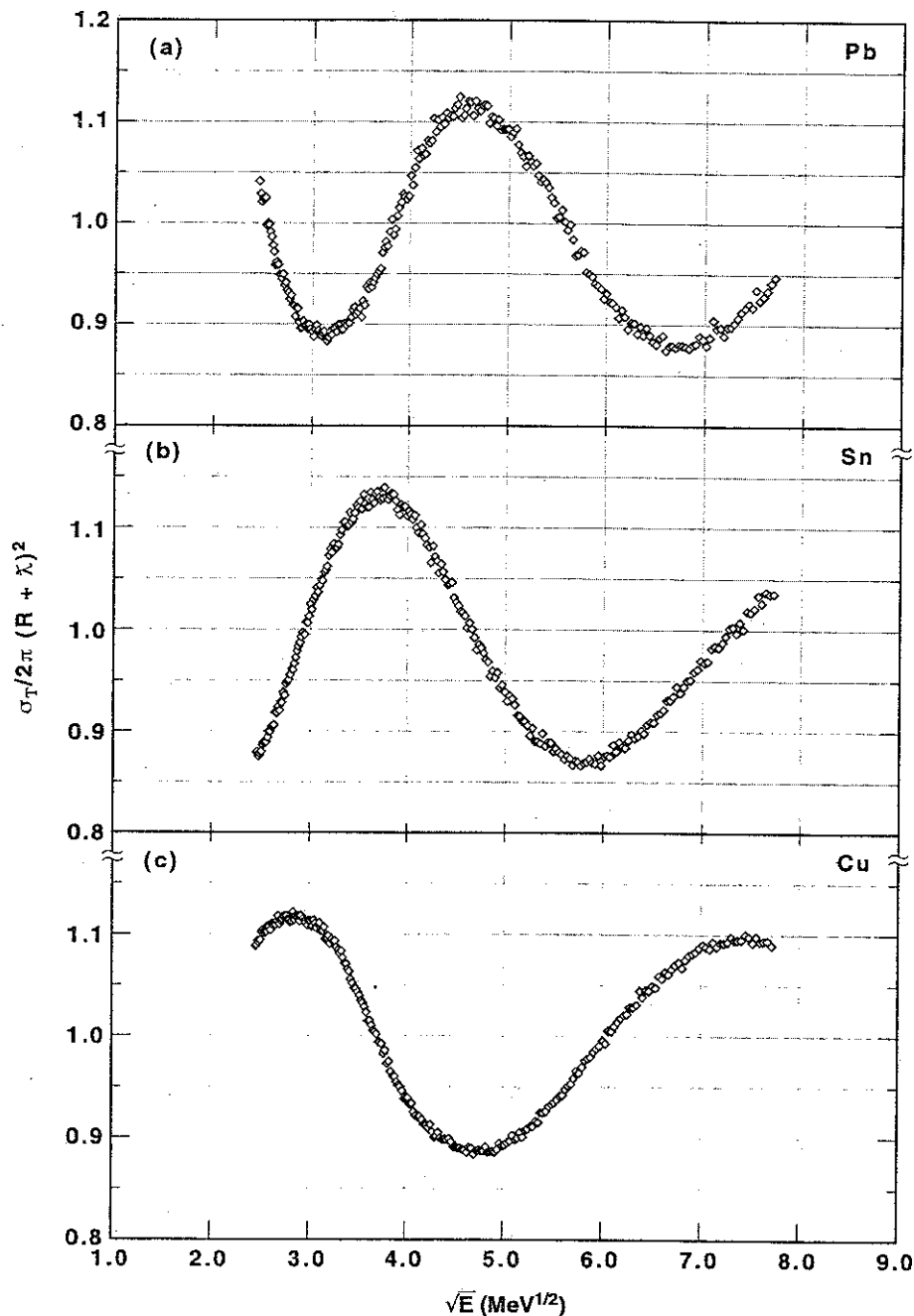


Fig. 1. Reduced neutron total cross section $\sigma_T/2\pi(R + \lambda)^2$ defined in Eq. (5) plotted against the square root of the neutron bombarding energy E for the energy range from 6 to 60 MeV. The reduced cross section oscillating about unity determines $r_0 = R/A^{1/3}$, and the amplitude of the oscillation determines α .

α to increase to ~ 0.13 for the lighter nuclei and to decrease to ~ 0.10 for the heavy nuclei. Figure 3 displays this general behavior as a function of atomic mass A . For a global approach for the energy range from 6 to 60 MeV, we recommend $\alpha = 0.18 - 0.013 A^{1/3}$, or the value of 0.115 ± 0.01 may be preferred.

If α is assumed to be due to just the absorption of the incoming wave, then we would expect a strong variation

of α with the nuclear radius. However, the averaging-out effect of the phases tends to mask any such variation, which implies that the averaging effect is dominant.

In our first analysis reported in Ref. 10, we found that β scales as $A^{1/3}$ as expected. Now we seek a universal form for $\beta/A^{1/3}$. The parameter β has its energy dependence constrained by the crossing points of the reduced cross section, for which $\cos \beta = 0$, and by the maxima

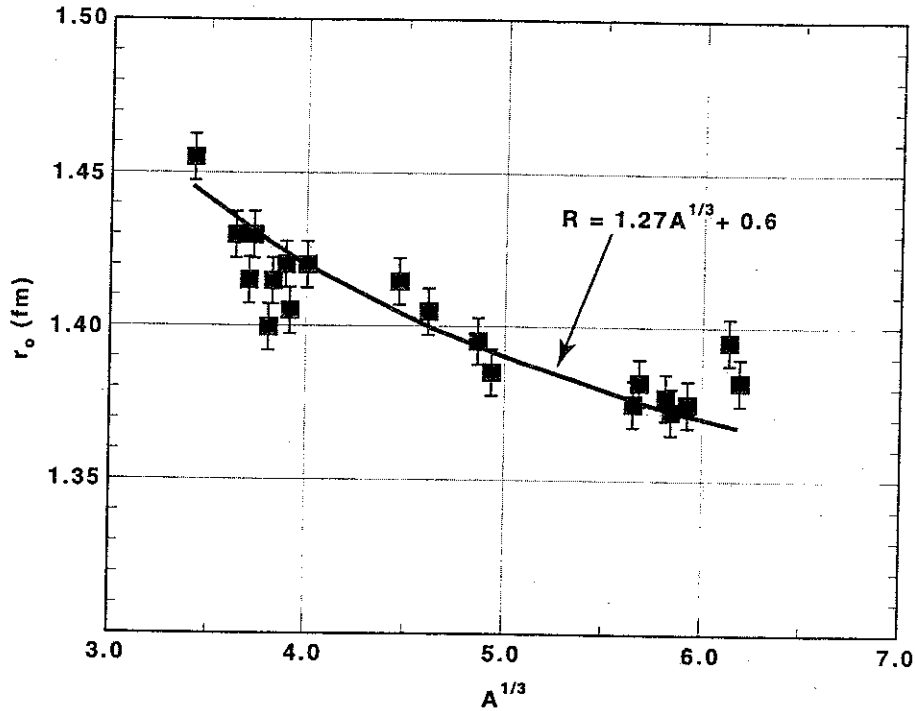


Fig. 2. Plot of r_0 and atomic mass A as determined from the reduction of the neutron cross sections from 6 to 60 MeV so that σ_r oscillates about unity [see Eq. (5)].

TABLE I

Variation of the Nuclear Radius $r_0 A^{1/3}$ as a Function of Atomic Number Z and Atomic Mass A

Element	Atomic Number Z	Nuclear Mass A	r_0 (fm)
Calcium	20	40	1.455 ± 0.005
Titanium	22	48	1.430
Vanadium	23	51	1.415
Chromium	24	52	1.430
Manganese	25	55	1.400
Iron	26	56	1.415
Cobalt	27	59	1.420
Nickel	28	60	1.405
Copper	29	64	1.420
Yttrium	39	89	1.415
Molybdenum	42	98	1.405
Indium	49	115	1.395
Tin	50	120	1.385
Tantalum	73	181	1.375
Tungsten	74	184	1.382
Gold	79	197	1.377
Mercury	80	200	1.373
Lead	82	208	1.375
Bismuth	83	209	1.375
Thorium	90	232	1.395
Uranium	92	238	1.382

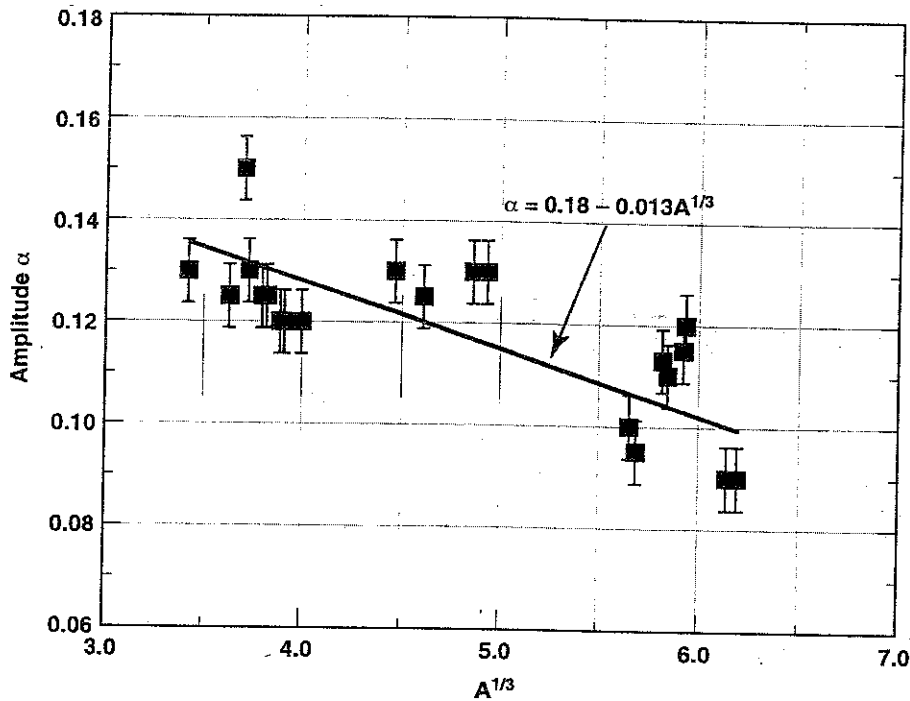


Fig. 3. Amplitude α plotted against atomic mass A as determined from the amplitude of the oscillations of the reduced cross sections such as plotted in Fig. 1. The shaded area indicates the region $\alpha = 0.115 \pm 0.01$.

and minima, for which $\cos \beta = -1$ and $+1$, respectively. To investigate the systematic dependence of the three fitting parameters a , b , and c [Eq. (4)] and to develop a universal form for β , we first examine the variation of β with energy for nuclei over a wide range of A values. Because β represents a phase shift, it is expected that β would be proportional to the nuclear radius. If the Ramsauer formula is to provide a fit to the total cross-section data, β/R should show a universal curve as a function of E ; i.e., plots of $\beta/A^{1/3}$ as a function of energy should fall on a universal curve that is independent of A .

Figure 4 illustrates the results of this analysis. The β values plotted were derived from the crossovers and maxima/minima of the reduced cross sections for six nuclei ranging from vanadium to uranium. The values of $\beta/A^{1/3}$ as a function of energy can be seen to lie on one universal curve. Equation (4) gives

$$\frac{\beta}{A^{1/3}} = c \cdot (\sqrt{a + bE} - \sqrt{E}) \quad (6)$$

In Fig. 4 we show a fit to this curve using standard optical model potentials and also a least-squares fit, where a , b , and c were allowed to vary. The standard optical model parameterization fails in two ways. First, the energy dependence of the optical potential depth is usually expressed as $V_0 - 0.3E$, where the energy-dependent term is a correction for the nonlocality of the real nuclear potential. For nominal values of V_0 , this implies that the

optical potential goes to zero at ~ 150 MeV, while measurements indicate this zero is at much higher energies, i.e., at ~ 250 MeV. Second, there is an additional contribution to the optical potential at low energies as a result of dispersion corrections. Thus, standard optical parameters do not have enough "curvature" at low energies and a wrong slope at high energies as shown in Fig. 4.

Although the parameterization is not unique, the simple form given in Eq. (6) provides a reasonable fit over the energy range from ~ 6 to 60 MeV, which is good to within ~ 1 to 2% for our least-squares parameters. These parameters are listed in Table II. The errors associated with the parameters are to be considered only as qualitative in nature; we found that the fitting parameters were highly correlated. This is similar to the VR^2 ambiguity found in optical model fits to neutron angular distributions. Figure 5 presents a sample of six targets ranging from calcium to lead using Eq. (6) and the global parameters listed in column 2 of Table II. Note that these are not fits to the cross-section data but are cross sections predicted by fitting the $\beta/A^{1/3}$ data of Fig. 4.

II.C. Fits with Extended Ramsauer Model

Inspection of the fits to the reduced cross-section data show a tendency for β to vary somewhat differently with E than given by the form of Eq. (6). Empirically we find that addition of a term proportional to the square of Eq. (6) gives an improved representation of the cross

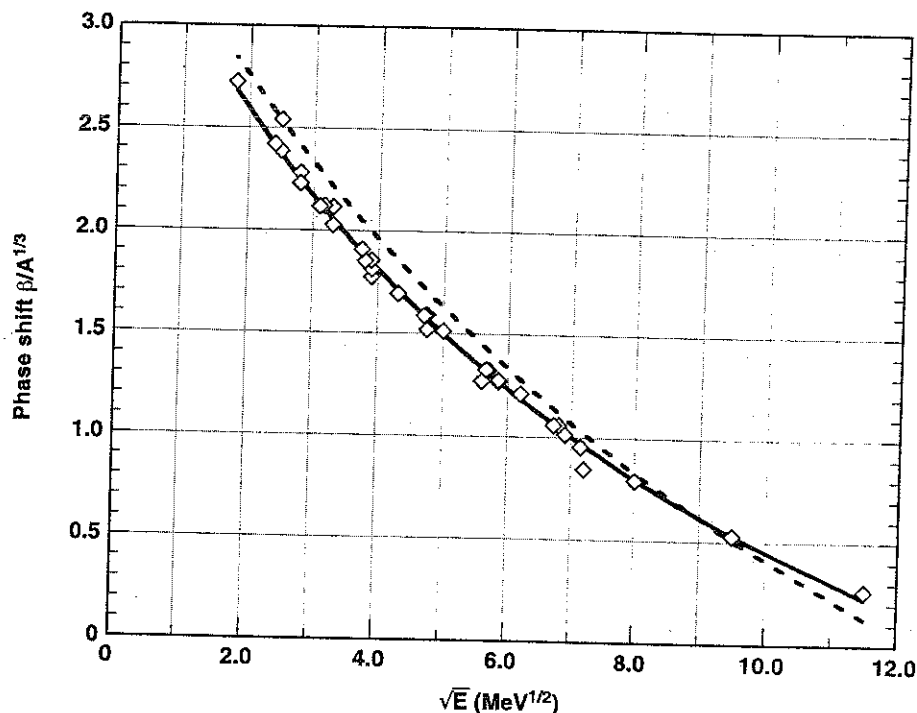


Fig. 4. Plot of phase shift $\beta/A^{1/3}$ as a function of the square root of the neutron bombarding energy E for achieving a universal fit for the three fitting parameters a , b , and c in Eq. (6). The solid curve is a fit to the data; the dashed curve uses standard optical model parameters listed in Table II. The data points are derived from the energy values at the maxima, minima, and ordinate crossings at $\sigma_T/2\pi(R + \lambda)^2 = 1$ of the measurements in Refs. 8 and 9 as plotted in Fig. 1.

TABLE II

Values of the Three Fitting Parameters a , b , and c Obtained from Fitting the Universal Form of β Given in Eq. (6)*

Parameter	Value First Global Fit	Value Standard Optical Model
a	35.0 ± 0.5	45.0
b	0.80 ± 0.01	0.70
c	0.62 ± 0.01	0.56

*The values listed are used in the "first" global fit to the data from 6 to 60 MeV using the basic Ramsauer model and also standard optical model parameters.

sections. This square term is introduced to compensate for an increased curvature at low energies. However, this change adds one additional parameter (k') to the expression for β , giving

$$\frac{\beta}{A^{1/3}} = c \cdot \{ [\sqrt{a + bE} - \sqrt{E}] + k' [\sqrt{a + bE} - \sqrt{E}]^2 \}. \quad (7)$$

A deviation from Eq. (6) is not really surprising. In the first place, the energy dependence of the potential

need not be strictly linear. Second, the approximations leading from the partial wave expansion of the scattering amplitude to the three parameters R , α , and β in Eq. (1) are not expected to be very accurate. Third, neither shell effects nor deformation have been included. The form of Eq. (7) is motivated partially by the energy dependence of the deviation in β obtained from data (see Sec. II.B) as function of energy from Eq. (6) but also by an attempt to increase β at low energies to match the dispersion correction to the optical potential known as the Fermi surface anomaly.

Figure 6 shows the comparisons of the cross sections obtained from Eq. (7) with the data. The parameters used in this comparison are listed in Table III, column 2. Excellent agreement is obtained within $\sim 1.5\%$ for nuclei heavier than copper. Somewhat larger discrepancies, 2.5 to 3%, are obtained for the nuclei with masses between calcium and copper. The fact that the deviations are so small is quite remarkable given that the fits are based on so few parameters.

II.D. Inclusion of Isospin

Section II.C pointed out that the quality of fits for nuclei lighter than copper was not as good as that for heavier nuclei. The form of the cross section for these lighter nuclei is such that it can be fit with a Ramsauer

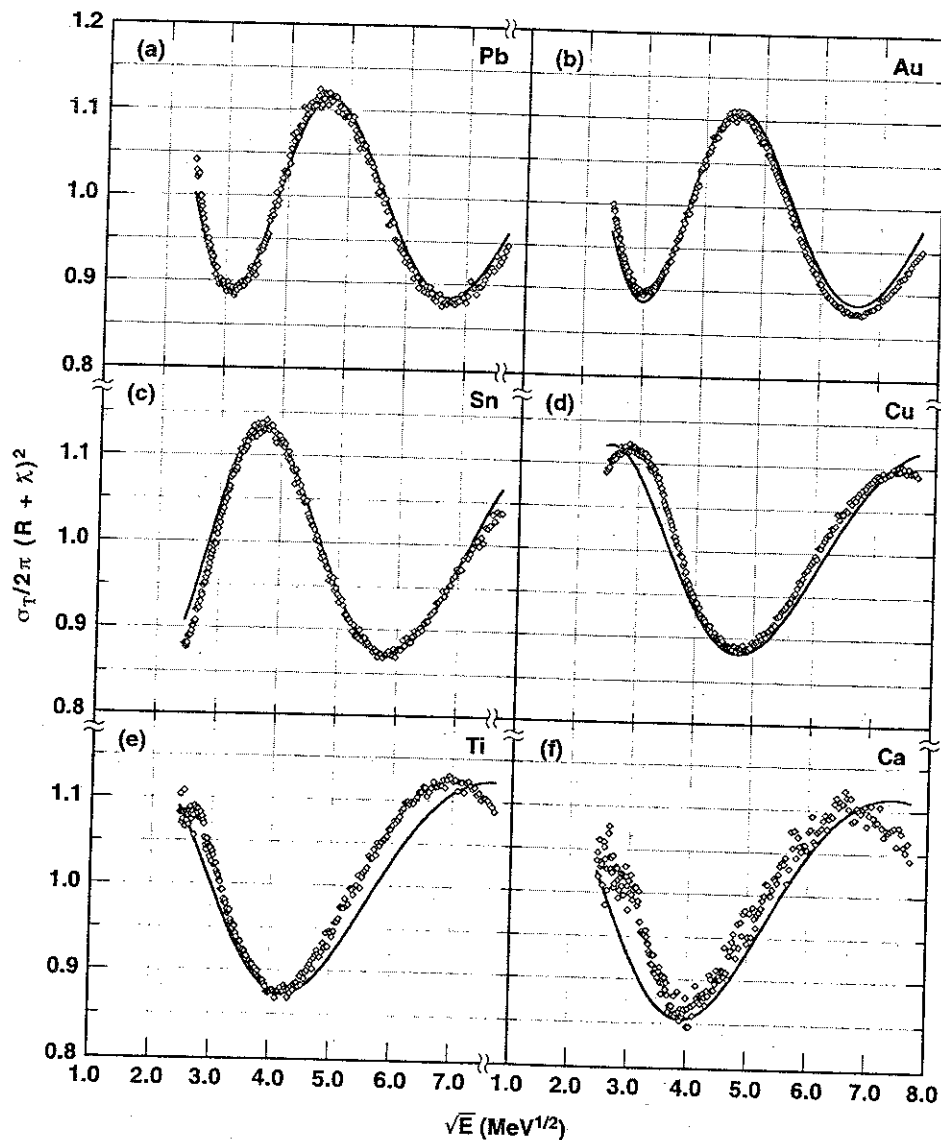


Fig. 5. First global fits of the basic Ramsauer model to the neutron cross sections from 6 to 60 MeV using Eq. (6) and the parameters for a , b , and c listed in Table II.

model, but the parameters needed differ somewhat from those obtained from the global fits to the heavier nuclei. One facet of the physics that has not been included to this point is the dependence of the potential on isospin. The lightest nuclei in the group studied here have isospin as small as 0, while the heaviest nuclei have isospin >20 . Since the isospin potential produces about a 5-MeV difference for these heavy nuclei, it needs to be included explicitly. Because of the large number of heavy nuclei among the group fitted, our global parameterization without isospin included will be biased toward values of the potential that are appropriate for large values of isospin.

We therefore carried out a search for parameters to express β in terms of nuclear potential that has a conventional isospin dependent term of $[(N-Z)/A]V_1$, where

$N-Z$ is the neutron excess and V_1 is the isospin potential ($V_1 \sim 24$ MeV). The number we obtained for V_1 from the fit is 21 MeV compared with the known value of 24 MeV. We use 24 MeV rather than introducing a new parameter. No effort was made to investigate the appropriateness of including isospin in α or R . This choice was made because the poor quality of fits for the light nuclei showed characteristics consistent with inappropriate energy dependence of β but did not show evidence of R or α values inconsistent with the systematics established by the heavier nuclei.

Figure 7 shows the results of these fits for lead, gold, tin, copper, titanium, and calcium. Note that the inclusion of an isospin term in the potential resulted in an improvement of the quality of fits for copper and the lighter

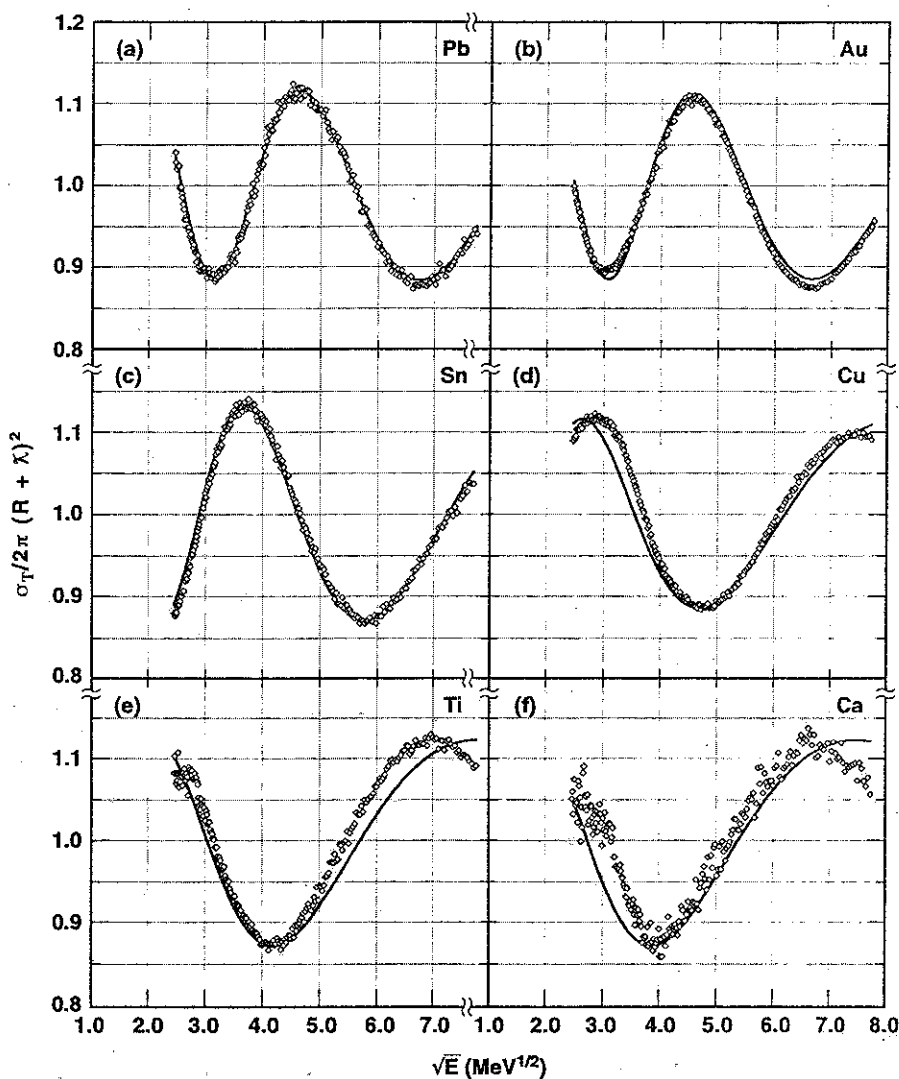


Fig. 6. Refined global fits of the extended Ramsauer model to the neutron cross sections from 6 to 60 MeV using Eq. (7) and the parameters for a , b , c , and k' listed in Table III, column 2.

TABLE III

Values of Three Fitting Parameters a , b , c , and k' Used for the Refined Global Fit, Using the Extended Ramsauer Model [Eq. (7)], and Modifications to Include Corrections for Isospin Used for the Corrected Global Fit* to the Data from 6 to 60 MeV

Parameter	Values Used for Refined Global Fit	Values Used for Corrected Global Fit
a	38.0 ± 0.5	$\left(43 - 24 \frac{N-Z}{A}\right)$
b	0.85 ± 0.01	$1.05 - 0.35 \left(1 - \frac{2(N-Z)}{A}\right)^a$
c	0.46 ± 0.01	0.46 ± 0.01
k'	0.070 ± 0.002	0.070 ± 0.002

*See Sec. II.D.

^aThe correct isospin dependence yields a much smaller correction, i.e., $1.00 - 0.22(1 - (N - Z)/2A)$.

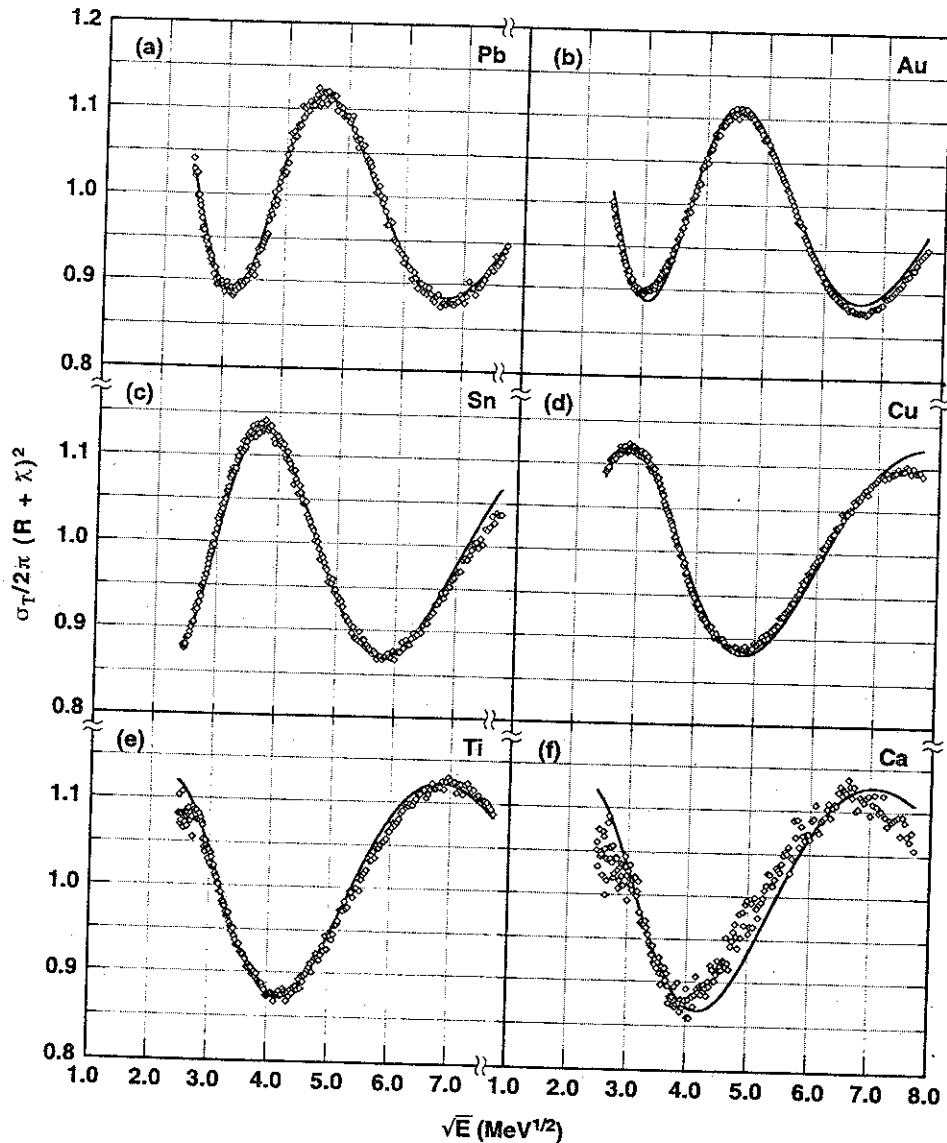


Fig. 7. Corrected global fits of the extended Ramsauer model (corrected for isospin) to the neutron cross sections from 6 to 60 MeV using Eq. (7) and the parameters for a , b , c , and k' listed in Table III, column 3.

nuclei, but did not cause the quality of fits to deteriorate for the heavier nuclei. Calcium is a special case with isospin equal to zero; the isospin correction improved the fit, but it is not quite as good as for the heavier nuclei. This is really not surprising because for calcium at 10 MeV, we only have three partial waves in our sum (see Ref. 7). We now have a parameterization that depends on E , A , N , and Z . It is quite impressive that this yields a formula that appears to be capable of representing the total neutron cross section for nuclei between calcium and uranium over the energy range of 6 to 60 MeV within 2%.

II.E. Possible Extension to Higher Energies

The excellent data sets^{8,9} extending to 600 MeV suggested to us that these fitting procedures be tried over the range of 6 to 600 MeV. Initial examination of the data over this range and a preliminary effort to follow the fitting procedure used below 60 MeV indicated that the energy dependence and magnitude of the cross sections could still be expressed in the form of Eq. (1). It became immediately clear, however, that the price for doing so was to introduce some energy dependence to both R and α . In addition, the β energy dependence appears to be

more complicated than was applied for the 6- to 60-MeV range. An extension to 120 MeV did seem feasible.

Because we are extending our calculations to ~100 MeV, we can no longer use the simple nonrelativistic description. At low energies, the relativistic correction can be expanded as a linear function of energy, and it represents a small shift along the energy axis. At higher energies, however, this leads to more complicated-looking equations but to no additional parameters. Thus, Eq. (6) in its relativistic form becomes

$$\beta/A^{1/3} = c \cdot \left(\sqrt{a + bE} \cdot \sqrt{1 + \frac{(a + bE)}{2mc^2}} - \sqrt{E} \cdot \sqrt{1 + \frac{E}{2mc^2}} \right) \quad (8)$$

The quantities a , b , c , and $A^{1/3}$ are the same as used in Eqs. (4) and (6) and were described earlier. The expression in the parentheses represents the relativistic form of the momentum-energy transformation, where mc^2 is the rest mass of the neutron.

We recall that we added a square term to Eq. (6) to compensate for an increased curvature at low energies (see Sec. II.C). Instead of adding the square term, we propose to use an alternate form that gives comparable results in fitting the data but eliminates the parameter k' . This newly proposed form comes from fitting the variation of the chord length of the path of the neutron inside the nucleus as discussed in Ref. 7. Fitting the length variations given in Table I of Ref. 7 yields a correction factor of $(1 - 0.02\sqrt{E})$ to be added to Eq. (8). It is to be noted that the introduction of this factor is a change in the average phase, not a change in normalization. Thus, in its relativistic form and with a chord length correction, the angle β becomes

$$\beta/A^{1/3} = (1 - 0.02\sqrt{E}) \times c \cdot \left(\sqrt{a + bE} \cdot \sqrt{1 + \frac{(a + bE)}{2mc^2}} - \sqrt{E} \cdot \sqrt{1 + \frac{E}{2mc^2}} \right) \quad (9)$$

The expression in the first set of parentheses on the right of Eq. (9) is the correction for the chord length variation, while the expression in the second set of parentheses, as pointed out earlier, represents the relativistic form of the momentum-energy transformation.

In our attempt to extend the application of the simple Ramsauer model, as given in Eq. (9), we plan to use the three fitting parameters a , b , and c as close as possible to those of the original global fit (listed in Table II). In this extension to 120 MeV, however, it becomes obvious that for the $(1 - \alpha \cos \beta)$ dependence to reproduce the experimental data, the values for both R and α can no longer be kept constant over the whole energy range. The

following slow energy dependence is imposed on the two parameters:

$$r_x = (1 - \mu\sqrt{E})r_{oc}A^{1/3} \quad (10)$$

and

$$\alpha_x = (1 - \nu\sqrt{E})\alpha_c \quad (11)$$

where

r_x, α_x = new energy-dependent values to be used for the extended range

r_{oc}, α_c = constants slightly larger than the r_0 and α used in the fitting for the limited range from 6 to 60 MeV

μ, ν = constants of the order of 0.01.

(For a listing, see Table IV.) The small correction factors are necessary: μ will cause the reduced cross section to oscillate about unity, even as we approach higher energies, and ν will correct for the "damping" of the oscillations of the normalized cross section at higher neutron energies. The small magnitude allows us to ignore the relativistic correction to the energy in these expressions.

The fact that r_0 should decrease with increasing energy is clear because at energies ~250 MeV, the nuclear radius should approach the nuclear matter radius as the nuclear potential goes to zero. With α we expect an increase due to the reduction of transit time in the nucleus, but this may be overcompensated by the cancellation of the various phases.

Using Eq. (9) and the global fitting parameters a , b , c , μ , and ν as listed in Table IV, we obtain the fits shown in Fig. 8. Inspecting the results for this extended

TABLE IV

Values of the Three Fitting Parameters a , b , and c Obtained from Fitting the Universal Form of β Given in Eq. (9) and Factors μ and ν for the Energy Dependences of R and α as Given in Eqs. (10) and (11), Respectively*

Parameter	Value
a	37.5 ± 0.5^a
b	0.80 ± 0.01^a
c	0.61 ± 0.01
μ	0.008
ν	0.010

*The values listed are used in the global fit to the data from 6 to 120 MeV using the basic Ramsauer model, in relativistic form and including a chord length correction.

^aThe values a and b for the light nuclei have been corrected for isospin; i.e., for copper the respective values are 40.0 and 0.75.

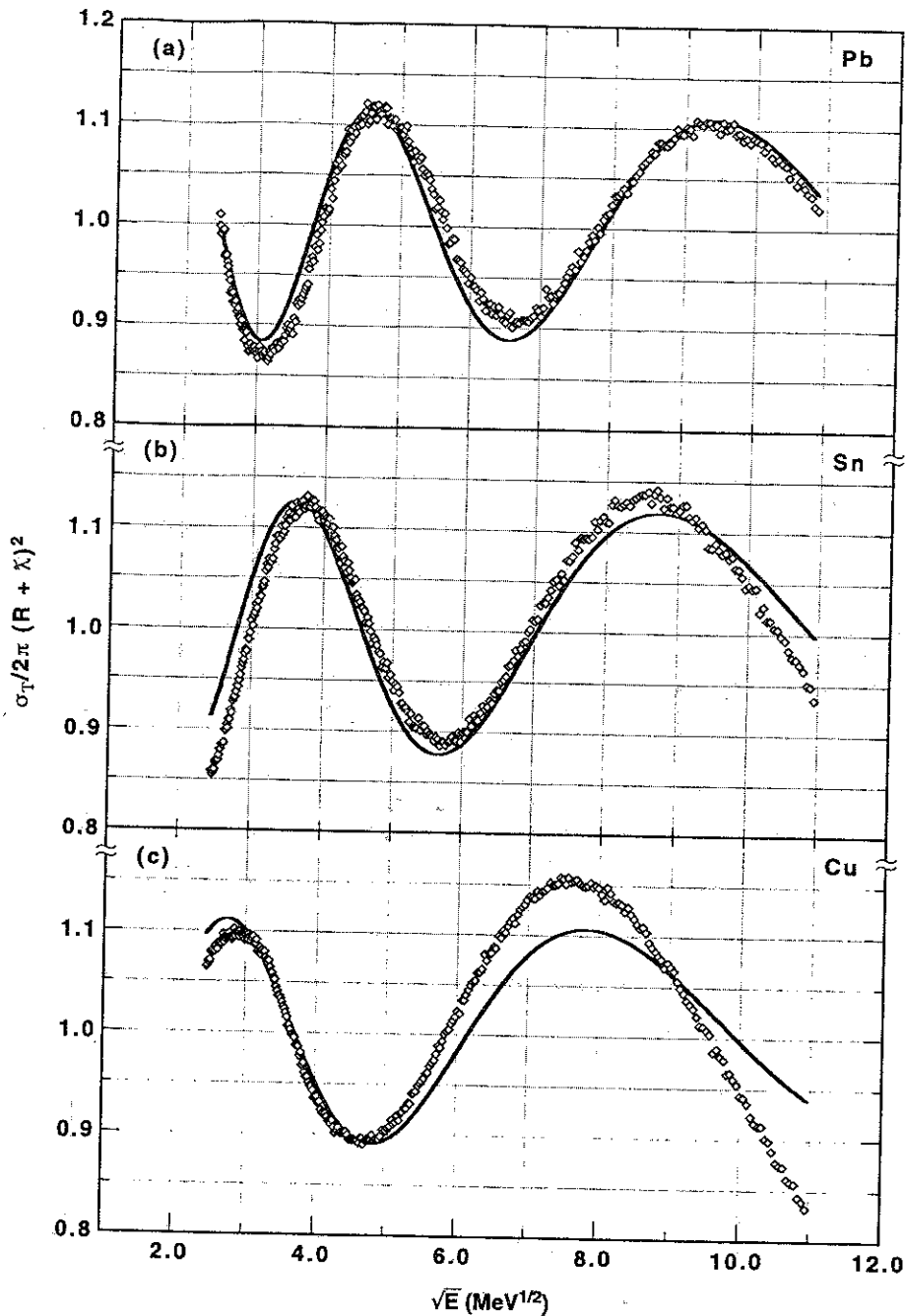


Fig. 8. Global fits of the basic Ramsauer model (in relativistic form and including a chord length correction) to the neutron cross sections from 6 to 120 MeV using Eqs. (9), (10), and (11) and the parameters for a , b , c , μ , and ν listed in Table IV.

energy range, we can conclude that the simple Ramsauer using global fitting parameters is still applicable, and it provides good fits to the total cross sections for energies from 6 to 120 MeV to an accuracy of 2 to 5% for the heavier nuclei and to $\sim 10\%$ for the lighter nuclei (copper and below). However, to achieve these fits, a small energy dependence had to be imposed on the nuclear radius and on the amplitude of the oscillations

of the reduced cross section. To obtain a better fit to the light nuclei, we had to give up our goal of achieving a universal curve for $\beta/A^{1/3}$. It would require at the very least a variation of our c parameter with A .

It is challenging to extend our study to energies beyond 150 MeV. This broader region not only includes the pion threshold but also spans the energy at which the nuclear potential changes from attractive to repulsive; thus,

additional complexity in the form of the energy variation of the parameters will not be surprising. We are in the process of an extensive study of the form of the parameterization for the Ramsauer expansion over the range from 60 to 600 MeV, which will be reported in a separate publication, as well as exploring Glauber calculations^{3,11} that should be more valid in the multihundred mega-electron-volt energy region.

III. CONCLUSIONS

Applying a simple Ramsauer model permits us to fit total neutron cross sections over a wide range of nuclei, covering the heaviest nuclei, such as thorium and uranium, down to light nuclei, such as titanium and calcium. Very good fits have been obtained using simple equations based on parameters with straightforward physical interpretations plus a small number of fitting parameters. For the energy range from 6 to 60 MeV, agreement between the Ramsauer model and the experimental data has been of the order of 1 to 1.5%, using refined global fits with all parameters kept constant over the whole energy range.

All the plots shown in Figs. 1 and 5 through 8 presented the reduced neutron cross section compared with

energy with the intent to emphasize any discrepancy between experimental data and our model calculations. However, to display the high quality of our fitting routine and to better appreciate our model's usefulness in describing neutron data, we present an example of our results in Fig. 9, where we chose to display the total cross section and energy, comparing the actual measured cross section and our model calculation. The excellent agreement between experiment and our model calculations is obvious.

The quality of the fit to the data at the higher energies (~ 100 MeV and above), however, has been found to deteriorate compared with the high quality achieved for the energy range from 6 to 60 MeV. Some improvement was provided by using relativistic kinematics. In addition, the need was found to introduce an energy dependence of the parameters R and α in the Ramsauer model. More detailed study of these energy dependences and the possibility of a modified energy dependence of β will be required to obtain optimal fits with the model up to 600 MeV as well as comparisons with Glauber model calculations to assess their usefulness.

In summary, we propose the Ramsauer model to be an excellent tool for fitting available neutron data and for estimating neutron total cross sections where no experimental data are available. Very good predictions with an accuracy of 1 to 1.5% can be expected in the energy

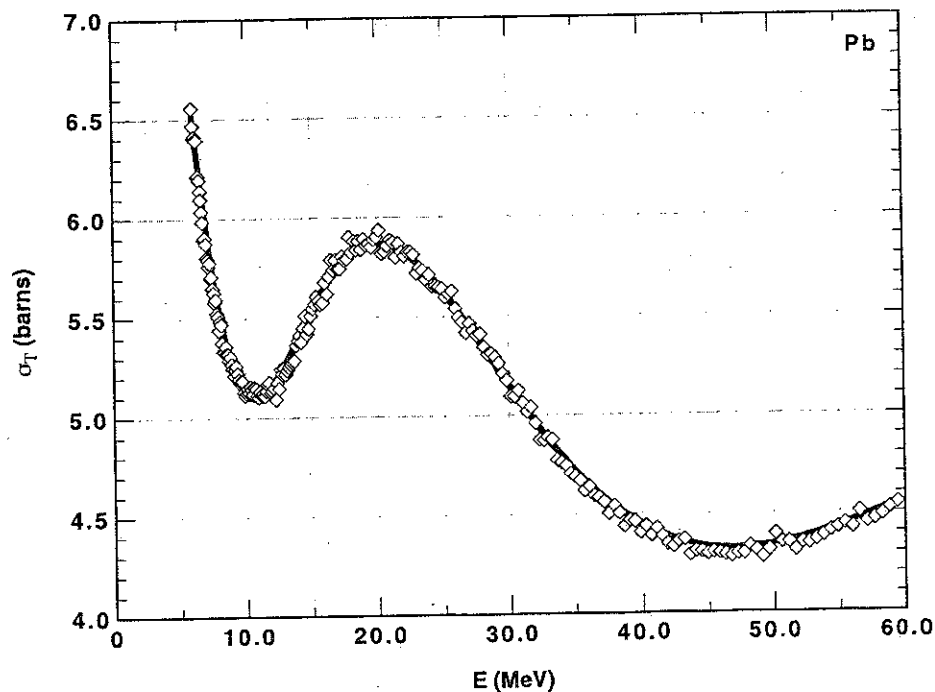


Fig. 9. Comparison of the measured total neutron cross sections for lead from 6 to 60 MeV with the refined global fit obtained by the extended Ramsauer model using Eq. (7) and the parameters for a , b , c , and k' listed in Table III, column 2. The experimental data and fitting parameters are identical to those of Fig. 6a.

range up to 60 MeV, using the refined global fits discussed in this paper. The quality of fit is sufficiently good to suggest that these systematics could be used to predict total neutron cross sections for elements that are not available as well as providing a convenient parameterization for those cross sections that have been measured in situations where a formula is more convenient than a large file of experimental data points. In addition, Camarda¹² suggested that the Ramsauer model might also provide predictions of angular distributions where no experimental data exist. Preliminary results for predicted angular distributions compared with experimental data appear encouraging. Further work in this area is in progress.

ACKNOWLEDGMENTS

This work was performed under the auspices of the U.S. Department of Energy by the Lawrence Livermore National Laboratory (LLNL) under contract W-7405-ENG-48. We also acknowledge valuable discussions with Harry S. Camarda and the general support of the LLNL Nuclear Data Group under Roger M. White.

REFERENCES

1. J. D. LAWSON, "A Diffraction Effect Illustrating the Transparency of Nuclei to High Energy Neutrons," *Phil. Mag.*, **44**, 102 (1953).
2. J. M. PETERSON, "Neutron Giant Resonances—Nuclear Ramsauer Effect," *Phys. Rev.*, **125**, 955 (1962).
3. V. FRANCO, "Quantitative Aspects of Neutron-Nuclear Interaction and the Optical Model," *Phys. Rev. B*, **140**, 1501 (1965).
4. K. W. MCVOY, "Giant Resonances and Neutron-Nuclei Total Cross Section," *Ann. Phys.*, **43**, 91 (1967).
5. C. R. GOULD, D. B. HAASE, L. W. SEAGONDOLLAR, J. P. SODERSTRUM, K. E. NASH, M. B. SCHNEIDER, and N. R. ROBERSON, "Spin-Spin Potential in $N_{\text{pot}} + {}^{27}\text{Al}_{\text{pot}}$ and the Nuclear Ramsauer Effect," *Phys. Rev. Lett.*, **53**, 2371 (1986).
6. D. G. FOSTER and D. W. GLASGOW, "Neutron Total Cross Sections, 2.5–15 MeV, I Experimental," *Phys. Rev. C*, **3**, 576 (1971); see also I. ANGELI and J. CSIKAI, "Total Neutron Cross Sections and the Nuclear Ramsauer Effect," *Nucl. Phys.*, **A158**, 389 (1970); see also I. ANGELI and J. CSIKAI, "Total Neutron Cross Sections and the Nuclear Ramsauer Effect," *Nucl. Phys.*, **A170**, 577 (1971).
7. S. M. GRIMES, J. D. ANDERSON, R. W. BAUER, and V. A. MADSEN, "Justification of a Simple Ramsauer Model for Neutron Total Cross Sections," *Nucl. Sci. Eng.*, **130**, 340 (1998).
8. R. W. FINLAY, W. P. ABFALTERER, G. FINK, E. MONTEI, T. ADAMI, P. W. LISOWSKI, G. L. MORGAN, and R. C. HAIGHT, "Neutron Total Cross Sections at Intermediate Energies," *Phys. Rev. C*, **47**, 237 (1993).
9. F. S. DIETRICH, W. P. ABFALTERER, R. C. HAIGHT, G. L. MORGAN, F. B. BATEMAN, and R. W. FINLAY, Private Communication (1997); see also "Recent Measurements of Neutron Total Cross Sections on a Wide Range of Targets from 5 to 600 MeV at LANSCE/WNR," *Proc. Int. Conf. Nuclear Data for Science and Technology*, Trieste, Italy, May 19–24, 1997.
10. R. W. BAUER, J. D. ANDERSON, S. M. GRIMES, and V. A. MADSEN, "Application of Simple Ramsauer Model to Neutron Total Cross Sections," *Proc. Int. Conf. Nuclear Data for Science and Technology*, Trieste, Italy, May 19–24, 1997.
11. A. BOHR and B. MOTTELSON, *Nuclear Structure*, Vol. I, p. 166, Benjamin, New York (1969).
12. H. S. CAMARDA, Private Communication (1997).

